NASA TECHNICAL MEMORANDUM

NASA TM X-1860

NASA TM X-1860

THE INFLUENCE OF CRACK LENGTH AND THICKNESS IN PLANE STRAIN FRACTURE TOUGHNESS TESTS

by Melvin H. Jones and William F. Brown, Jr.

Lewis Research Center

Cleveland, Ohio

NATIONAL AERONAUTICS AND SPACE ADMINISTRATION • WASHINGTON, D. C. • AUGUST 1969

NASA TM X-1860

THE INFLUENCE OF CRACK LENGTH AND THICKNESS IN PLANE STRAIN FRACTURE TOUGHNESS TESTS

By Melvin H. Jones and William F. Brown, Jr.

Lewis Research Center
Cleveland, Ohio

NATIONAL AERONAUTICS AND SPACE ADMINISTRATION

For sale by the Clearinghouse for Federal Scientific and Technical Information
Springfield, Virginia 22151 – CFSTI price $3.00

ABSTRACT

It is shown that K_{Ic} values determined in accordance with the present ASTM E-24 Proposed Test Method for Plane Strain Fracture Toughness of Metallic Materials can vary moderately within the specimen size and geometric limitations imposed by the Test Method. The magnitude of these variations will depend on the material properties and would be increased by relaxation of the size requirements. The possibility of employing subsized specimens for screening materials regarding their plane strain fracture toughness was explored as well as several methods for relating K_{Ic} values to uniaxial tensile data.

THE INFLUENCE OF CRACK LENGTH AND THICKNESS IN PLANE STRAIN FRACTURE TOUGHNESS TESTS

by Melvin H. Jones and William F. Brown, Jr.

Lewis Research Center

SUMMARY

Results are presented from a systematic investigation of the influence of crack length and specimen thickness on the fracture properties of 4340 steel bend specimens heat treated to yield strength levels between 180 and 213 ksi (1240 and 1467 MN/m^2). It is shown that plane strain crack toughness (K_{Ic}) values determined in accordance with the present ASTM E-24 Proposed Test Method for Plane Strain Fracture Toughness of Metallic Materials can vary moderately within the specimen size and geometric limitations imposed by the Test Method. The magnitude of these variations will depend on the material properties and would be increased by relaxation of the size requirements.

The possibility of employing subsized specimens for screening materials regarding their plane strain fracture toughness was explored as well as several methods for relating K_{Ic} values to uniaxial tensile data. The results indicated that use of subsized specimens with the E-24 Test Method does not constitute a useful screening procedure. For steels subject to single aging or tempering reactions it appears that the relation $K_{Ic} \sim \sigma_Y^{-m}$ may be useful for estimating K_{Ic} values. However, on the basis of present knowledge, it is not possible to calculate K_{Ic} with useful accuracy from uniaxial tensile data alone.

INTRODUCTION

The recently issued ASTM E-24 Proposed Method of Test for Plane Strain Fracture Toughness of Metallic Materials (ref. 1) incorporates two basic features: specimen size requirements, which arise from the necessity of restricting the application of linear elastic fracture mechanics to situations of small scale yielding (ref. 2), and an arbitrary procedure for selecting the load (ref. 3), which arises from the absence of a clearly defined abrupt onset of fracture. It is not generally recognized that these features can

result in a variation of valid K_{Ic} values due to variations in specimen size permitted by the E-24 Test Method.

This geometric influence may be illustrated by figure 1 which shows schematic load-displacement curves for valid tests on a tough and a brittle alloy using two specimens having the same thickness and different crack lengths but otherwise of standard proportions. For these conditions, K_I would be proportional to $P/\sqrt{a}$, and this ratio is used as the ordinate of figure 1. The secant lines OS represent a 5-percent change in the slope of the linear portion OA of the records. This change in slope corresponds approximately to the 2-percent apparent extension of the initial crack specified in the ASTM

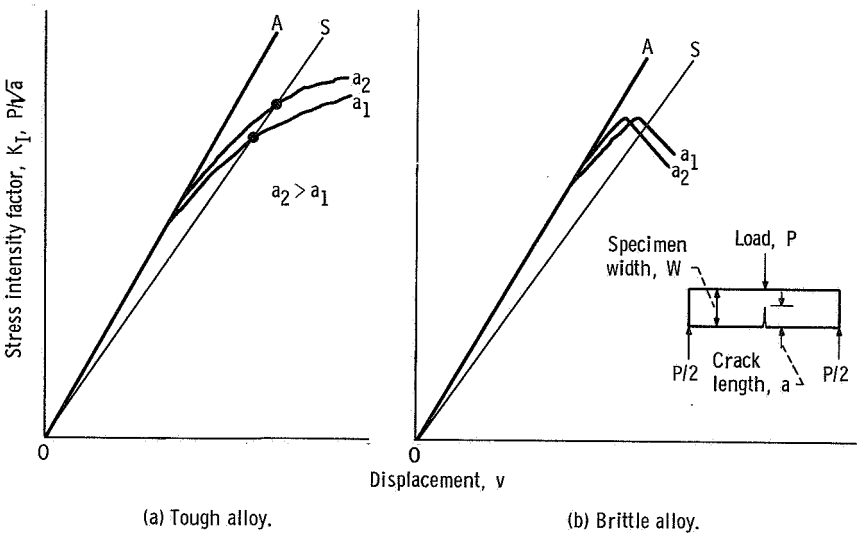

Figure 1. - Schematic load-displacement curves for two specimens of different crack lengths with equal thickness and crack length to specimen width ratio (a/W) illustrating effect of crack length on plane strain fracture toughness (K_{Ic}) for a tough and a brittle alloy.

E-24 Test Method. For the tough alloy, the intersection of this line with the test record establishes the $P_Q/\sqrt{a}$ value used to calculate K_{Ic}. For the brittle alloy, the maximum loads occur between OA and OS and are therefore used to calculate K_{Ic}. Note that the tough alloy shows crack extension under rising load beyond the points of intersection of the secant line with the load-displacement record. In these circumstances, the curves for $P/\sqrt{a}$ as a function of v would have to be identical in the range of small crack extension if K_{Ic} is to be independent of the initial crack length. This would require $\Delta a/W$ to be independent of the initial crack length. This behavior is most unlikely and, as shown later, the absolute crack extension Δa is nearly independent of the initial crack length. Consequently, at the same $P/\sqrt{a}$ value, the specimen of the tough alloy with the longer initial crack a_2 will represent a smaller $\Delta a/W$, or conversely the same per-

centage apparent crack extension in the specimen with the longer initial crack a_1 will require a higher load. Thus, the measured K_{Ic} values can increase with the initial crack length of the specimen. The magnitude of this effect will depend on the shape of the load-displacement record as controlled by both the thickness of the specimen and the material properties. For the brittle alloy where there is a maximum load between OA and OS, the effect of crack length on K_{Ic} will be negligible.

The geometric effects described can, under certain conditions, produce an apparent constancy of K_{Ic} over a range of crack lengths and specimen thicknesses outside those established by the size requirements and thus lead to the erroneous conclusion that the size requirements can be relaxed. Furthermore, geometric effects on the measured toughness values can be particularly important when there are large deviations from the size requirements or proportions of the ASTM recommended specimens, such as might be encountered in use of subsized specimens for "screening" tests.

The purpose of the present investigation was to determine the magnitude of these geometric effects that could be encountered in plane strain fracture toughness tests on a commonly used high-strength steel. Systematic tests were made to determine the influence of crack length and thickness in bend tests of a SAE 4340 steel. Most of these tests were performed on specimens of standard proportions (i.e., $0.45 < a/W < 0.55$ and $2 < W/B < 4$). In addition, a limited number of tests was made on specimens having a/W and W/B ratios outside the ranges permitted by the ASTM Test Method. Comparison of the 4340 data with that from another investigation (ref. 4) of maraging steel provided some indication of the difficulties which could be encountered when using subsized specimens for rating materials regarding their plane strain fracture toughness. The results of this investigation were also useful in a study of the relation between tensile properties and K_{Ic} proposed by Hahn and Rosenfield (ref. 5).

MATERIAL AND SPECIMEN PREPARATION

The material AISI E4340 aircraft quality steel was received in the form of 1-inch-(2.5-cm-) thick hot-rolled and annealed plates (36 by 60 in. (81 by 152 cm)) having the composition given in table I.

Bend Specimens

Full thickness bend specimen blanks were cut from one plate (RW direction) with the positions being randomized in respect to the plate width and the required length. (An analysis of the fracture toughness data did not reveal any effect of specimen location

TABLE I. - COMPOSITION OF AISI E4340 STEEL[a]

Heat number	Composition,[b] wt. %							
	C	Mn	P	S	Si	Ni	Cr	Mo
Lukens Bo 315	0.42	0.71	0.010	0.012	0.25	1.77	0.80	0.23

[a]Mill annealed, 1550° to 1600° F (1117 to 1144 K), 1 hr; furnace cooled to below 800° F (700 K).
[b]Furnished by supplier.

within the area of the plate used.) Where possible, these blanks were machined to the standard chevron notch and integral knife edge configuration given in the ASTM E-24 Test Method. Where the crack length to thickness ratio was insufficient to permit use of the chevron notch, the slot was terminated in a straight across 60° V-notch with a 0.0005-inch (0.13-μm) maximum root radius. Specimens with this slot configuration also had integral knife edges.

Specimen blanks with crack starter slots were heat treated in a neutral salt bath (1550° F (1117 K), 1/2 hr, oil quench + temper, 1 hr), and then fatigue cracked in cantilever bending with K_{max} (estimated from three-point bend specimen K calibration) not exceeding 27 ksi $\sqrt{in.}$ (29.7 $MNm^{-3/2}$) and $\Delta K/K_{max}$ of about 0.95. The number of cycles necessary to extend the fatigue crack beyond the tip of the crack starter was in all cases greater than 50 000. Specimens less than 1 inch (2.5 cm) thick were cut from the full thickness fatigue cracked blanks using a power hacksaw and then ground on their side surfaces. Any effect of specimen location with respect to the center of the plate thickness was within the scatter of data.

Smooth Specimens

Smooth tensile specimens with a 0.3-inch- (7.6-mm-) diameter test section and 2-inch (5.1-cm) gage length were cut from the broken halves of 0.5-inch- (1.3-cm-) thick bend specimens with the longitudinal axis in the rolling direction.

TEST PROCEDURE

The geometric conditions investigated using bend specimens are summarized in table II. The basic test program was confined to specimens tempered at 750° F (672 K). All these specimens met the size requirements in terms of crack length and had an

TABLE II. - GEOMETRIC CONDITIONS INVESTIGATED

[All tests in RW direction.]

Temper temperature		Conventional yield strength		Initial crack length, a_o		Specimen width, B		Specimen thickness, W		Ratio of crack length to specimen width, a/W	Ratio of specimen width to thickness, W/B
				in.	mm	in.	mm	in.	mm		
^{o}F	K	ksi	MN/m^2								
600	589	232	1598	1.0	25	1.0	25	2.0	51	0.5	2
750	672	213	1467	.27	6.9	0.05 to 0.50	1.25 to 12.7	.55	13.9	.5	11 to 1.1
				.50	12.7	0.055 to 0.98	1.39 to 24.9	1.0	25	.5	18 to 1.0
				1.1	27.9	0.055 to 1.0	1.39 to 25	2.4	60.9	.5	44 to 2.4
850	728	198	1364	1.1	27.9	1.1	27.9	2.2	55.8	.5	2
925	769	182	1253	0.33 to 1.5	8.4 to 38	1.0	25	2.0	51	0.17 to 0.75	2
				0.30 to 1.4	7.6 to 36	.1	2.5	2.0	51	0.15 to 0.7	20

a/W = 0.5. An additional series of tests was run for a 925^{o} F (769 K) temper in order to investigate conditions in which both thickness and crack length differed greatly from the requirements for a valid fracture toughness test. A limited number of tests was made on specimens tempered at 600^{o} and 850^{o} F (589 and 728 K) in order to establish a relation between K_{Ic} and tempering temperature for this plate of 4340 steel.

Bend specimens were tested in accordance with the procedures outlined in the ASTM E-24 Test Method. Those having width to thickness ratios of 10 or larger were provided with lateral support at the span rollers by clamping flat pieces of metal with sheet polytetrafluoroethylene separators to the specimen at this location. Load-deflection records were produced by an autographic recorder being fed by the output of the load cell and the clip-in displacement gage. For some tests, the specimen was also monitored with an acoustic pickup whose output could be correlated with the load (ref. 6).

Load-strain curves were obtained for the smooth specimens using a conventional 0.5-inch (1.3-cm) gage length extensometer in conjunction with the load-strain recorder of the tensile machine. This information was supplemented by micrometer measurements of the minimum specimen diameter at suitable load increments up to fracture. These measurements overlapped the extensometer readings.

ANALYSIS OF DATA

Bend Specimens

It is helpful in understanding the effects of the geometric variables if the load-displacement records are converted to curves for K as a function of Δa or crack

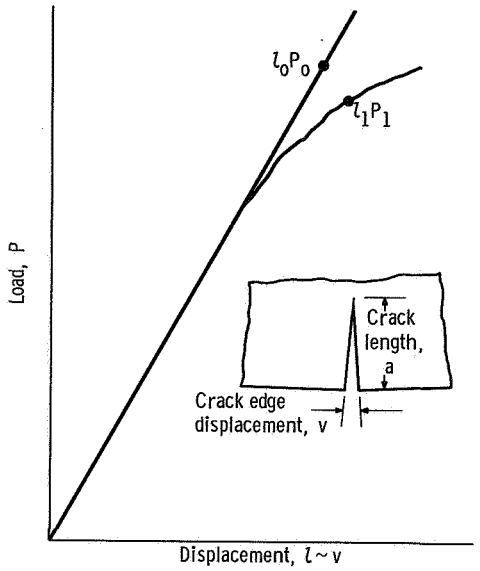

Figure 2. - Schematic autographic load-displacement plot for bend specimen illustrating quantities measured for calculation of curves for stress intensity factor as function of crack extension.

growth resistance, where Δa is the apparent crack growth increment[1] from the initial crack length a_o. This conversion was made for the specimen series tempered at 750° F (672 K). The procedure may be illustrated by reference to figure 2, which shows an autographic record with the vertical scale converted to load. The clip gage output is displayed on the horizontal scale and can be converted to displacement through a calibration factor derived from the slope of the linear (elastic) portion of the record and a_o (measured after the test). The relation between displacement, load, and relative crack length a/W is usually given in the form of a dimensionless displacement factor (ref. 2)

$$\frac{vEB}{P} = F \tag{1}$$

where B is the thickness, E the elastic modulus, F a function of a/W, and the other terms are as defined in figures 1 and 2. An equation for F(a/W) is given in appendix A.

The calibration factor for displacement is then

[1]The actual crack growth increment will be generally somewhat less than the apparent value determined from an analysis of the load-displacement records. This difference arises from the contribution of crack tip plastic flow to the measured displacements. Also, the actual crack front is slightly curved outward in the direction of crack propagation. Differences between apparent and actual crack extensions arising from these sources are not significant to the type of analysis made in this investigation.

$$C = \frac{v_o}{l_o} = \frac{F\frac{a_o}{W}}{EB}\frac{P_o}{l_o} \tag{2}$$

where v_o is the displacement corresponding to the scale distance l_o at load P_o on the linear portion of the record. Then, at another load P_1, $v_1 = l_1 C$, where l_1 is the scale distance corresponding to P_1. Therefore,

$$\frac{v_1 EB}{P_1} = \frac{l_1 CEB}{P_1}$$

Substituting from equation (2) for C gives

$$\frac{v_1 EB}{P_1} = \frac{l_1}{P_1} F\frac{a_o}{W}\frac{P_o}{l_o} = \frac{l_1}{P_1}\alpha \tag{3}$$

The conversion coefficient α is dependent only on the slope of the linear portion of the record and $F(a_o/W)$. The value of $\Delta a = a - a_o$, corresponding to a given point on the load-displacement curve, may then be determined with the aid of equation (1) for which a polynominal form is given in appendix A. As described in appendix B, the uncertainties of this analysis make the initial portion of the crack-growth-resistance curve impossible to determine with useful accuracy. However, these uncertainties are not troublesome in respect to establishing the general effects of crack length and thickness on the measured toughness values.

The K_I values were computed using the following expression for three-point bending with a span to width ratio of 4

$$K_I = Y\frac{6Ma^{1/2}}{BW^2}$$

where Y is a function of a/W, and M is the applied bending moment. In standard K_{Ic} tests, the a value would be the initial crack length. However, for this analysis, the a values were calculated as described previously, and, therefore, the computed values of K_I reflect changes in crack length as well as load.

The autographic plots were reduced to crack-growth-resistance curves point by point with the points distributed to establish best the curves in the region of small crack extensions. For the thickest specimens, the load-displacement curves sometimes were characterized by several large steps (fig. 3), as contrasted with the relatively smooth behav-

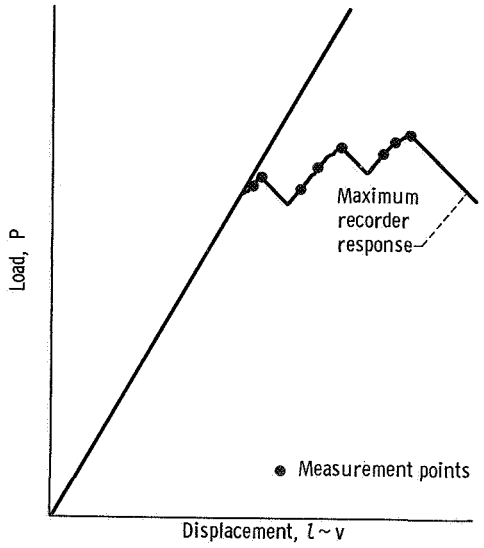

Figure 3. - Stepped-type autographic load-displacement plot showing measurement points for calculation of stress intensity factor as a function of crack extension.

ior shown in figure 2. These steps are caused by abrupt advances of the crack accompanied by unloading. During unloading, the rate of change of load and displacement exceeded the response capability of the autographic recorder. Consequently, the unloading trace has no meaning; its slope is only a function of the relative response speeds of the X and Y axes pens. Therefore, as indicated in figure 3, these types of records were analyzed by considering only the maximum load points or those on the rising load portion of the record.

Smooth Specimens

True stress and natural longitudinal plastic strain values were obtained by reducing the load-strain plots and micrometer measurements of diameters by the method outlined in appendix C. Where the extensometer and diameter change measurements overlapped, the longitudinal strain values derived from each agreed within about 2 percent. The true stress and natural plastic strain data were plotted on linear coordinates and on logarithmic coordinates in an attempt to define a strain-hardening index which would be useful in checking proposed correlations between K_{Ic} and uniaxial tensile properties. As discussed later, the necking strain was obtained by graphic differentiation of the true-stress - natural-strain curves.

RESULTS FOR EFFECTS OF THICKNESS AND CRACK LENGTH

This section presents results from two series of tests:

(1) A series with specimens tempered at 750° F (672 K) having various thicknesses and crack lengths meeting the present size requirements and an $a/W \approx 0.5$

(2) A series with specimens tempered at 925° F (769 K) having crack lengths and thicknesses substantially less than those corresponding to the size requirements

Crack-Growth-Resistance Curves for 750° F (672 K) Temper Series

Typical curves for K as a function of Δa derived from the load-displacement records are shown in figure 4 for specimens of three different thicknesses. For the crack lengths investigated, the crack-growth-resistance curves are identical within the limits of scatter as represented by the bands shown in this figure. As mentioned in the previous section, the Δa values lack useful precision in the region near the origin, as indicated by the dashed lines in figure 4. The inset in each part of the figure characterizes the type of load-displacement plot obtained for the particular specimen thickness tested. The vertical lines represent Δa values corresponding to 2 percent crack extension for each of the crack lengths investigated, and the intersections of these lines with the curves for K as a function of Δa give the corresponding K_Q values.[2]

It is evident from figure 4 that the K_Q value increases with crack length and that the magnitude of this effect depends on the shape of the crack-growth-resistance curve as influenced by specimen thickness. The thickest specimens (fig. 4(a)) exhibit the flattest resistance curves and the smallest effects of crack length. Reducing the specimen thickness results in curves with increasing slopes and larger effects of crack length on K_Q. For the thinnest specimens (fig. 4(c)), these effects represent a spread in K_Q of nearly 50 percent. This influence of thickness on the crack length effect might be expected because, as thickness is reduced, transverse constraints are relieved by crack tip plastic flow. This results in increased resistance to crack propagation and larger amounts of stable crack extension. These effects are reflected in the load-displacement records (see insets in fig. 4) as increased deviations from linearity before maximum load and in the crack-growth-resistance curves as an increase in slope.

[2] In an actual fracture toughness test, the K_Q value will be based on the initial crack length and consequently would be lower than that obtained from the curves for K as a function of Δa. This difference will increase with the absolute crack extension and would amount to a maximum of about 4 percent for the conditions represented in fig. 4.

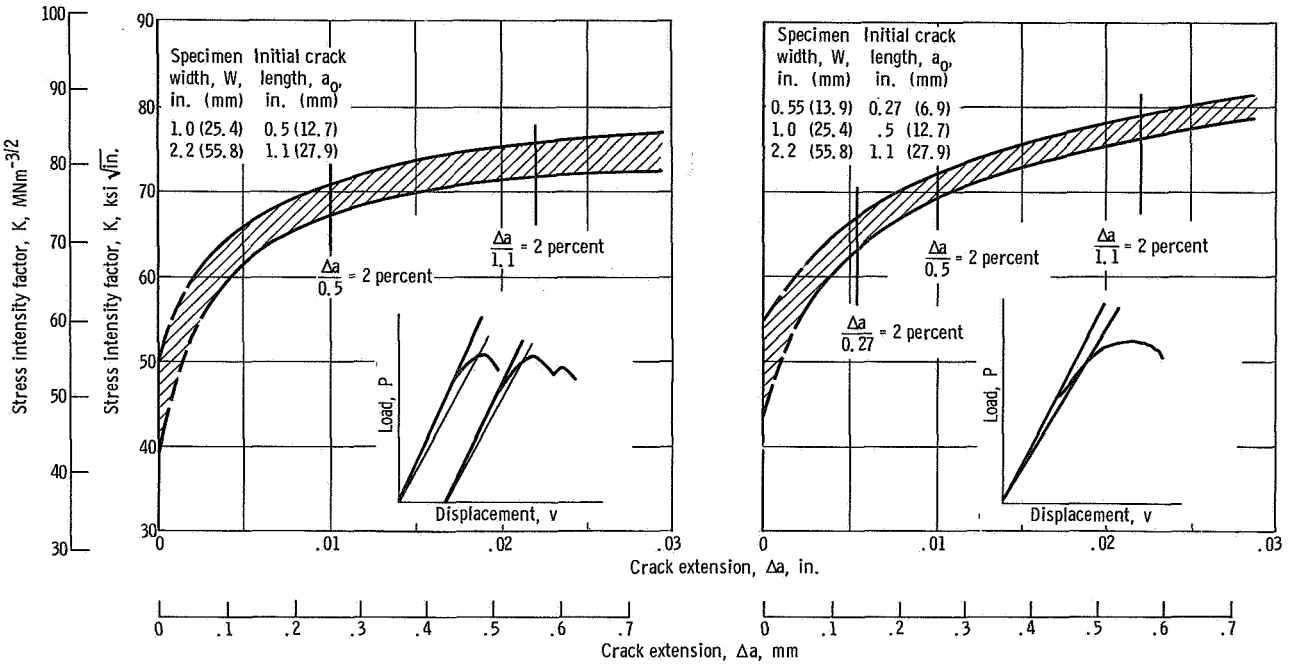

(a) Bend specimen thickness, 1 inch (25 mm).

(b) Bend specimen thickness, 0.27 inch (6.9 mm).

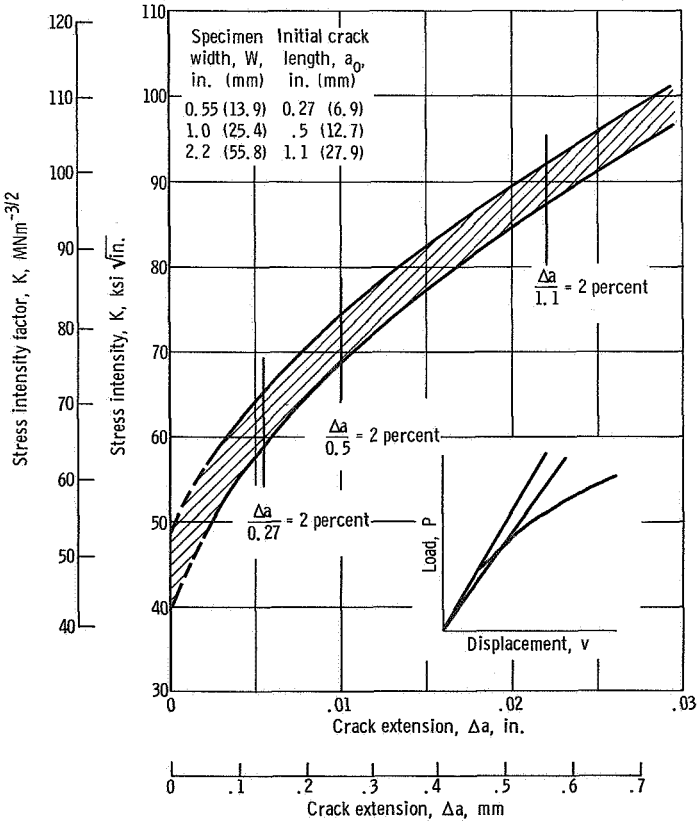

(c) Bend specimen thickness, 0.05 inch (1.3 mm).

Figure 4. - Crack-growth-resistance curve for 4340 steel tempered at 750° F (672 K) for 1 hour. Conventional yield strength, 213 ksi (1467 MN/m^2).

Some of the consequences of the interaction between the crack length and thickness effects on K_Q can be seen from figure 5, which combines the average curves for the scatterbands shown in figure 4. If the different thickness specimens had crack lengths of 0.5 inch (13 mm), 2-percent crack extension would represent a Δa of 0.01 inch (0.25 mm) and essentially no effect of thickness on K_Q would be observed. On the other hand, if the crack length was 1 inch (25 mm), 2-percent crack extension would represent a Δa of 0.02 inch (0.51 mm) and K_Q would increase as the thickness decreased. The opposite effect of thickness on K_Q would be observed for a crack length of 0.27 inch (6.9 mm). These effects of geometry on K_Q are quite large for the conditions investigated, where there are substantial deviations from the specimen size requirements and proportions recommended in the ASTM Test Method. An estimate of the magnitude of the geometric effects for valid K_{Ic} tests may be made by examining the K_Q values obtained for the entire range of specimen thicknesses tested.

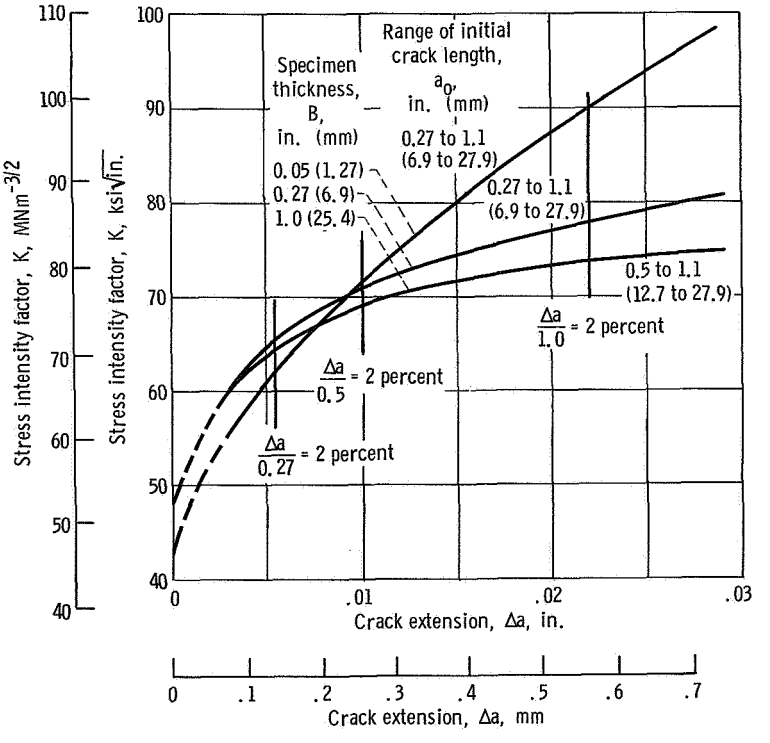

Figure 5. - Composite of crack-growth-resistance curves for 4340 steel tempered at 750° F (672 K) for 1 hour as determined using bend specimens of three thicknesses. Conventional yield stress, 213 ksi (1467 MN/m^2).

K_Q Values for 750° F (672 K) Temper Series

The K_Q values obtained in accordance with the ASTM E-24 Test Method (based on initial crack lengths) are shown in figure 6. These data represent a wide range of thicknesses for specimens having initial crack lengths of 0.27, 0.5, and 1.1 inch (6.9, 13, and 28 mm). Those tests failing to satisfy the E-24 Test Method check procedure for at least 1 percent actual crack extension at K_Q are designated "excess plasticity." The thickness corresponding to the size requirement $B = 2.5(K_{Ic}/\sigma_{YS})^2 = 0.27$ inch (6.9 mm) is marked in each figure. This thickness value is based on a $K_{Ic} = 70$ ksi$\sqrt{\text{in.}}$ (77 $MNm^{-3/2}$).

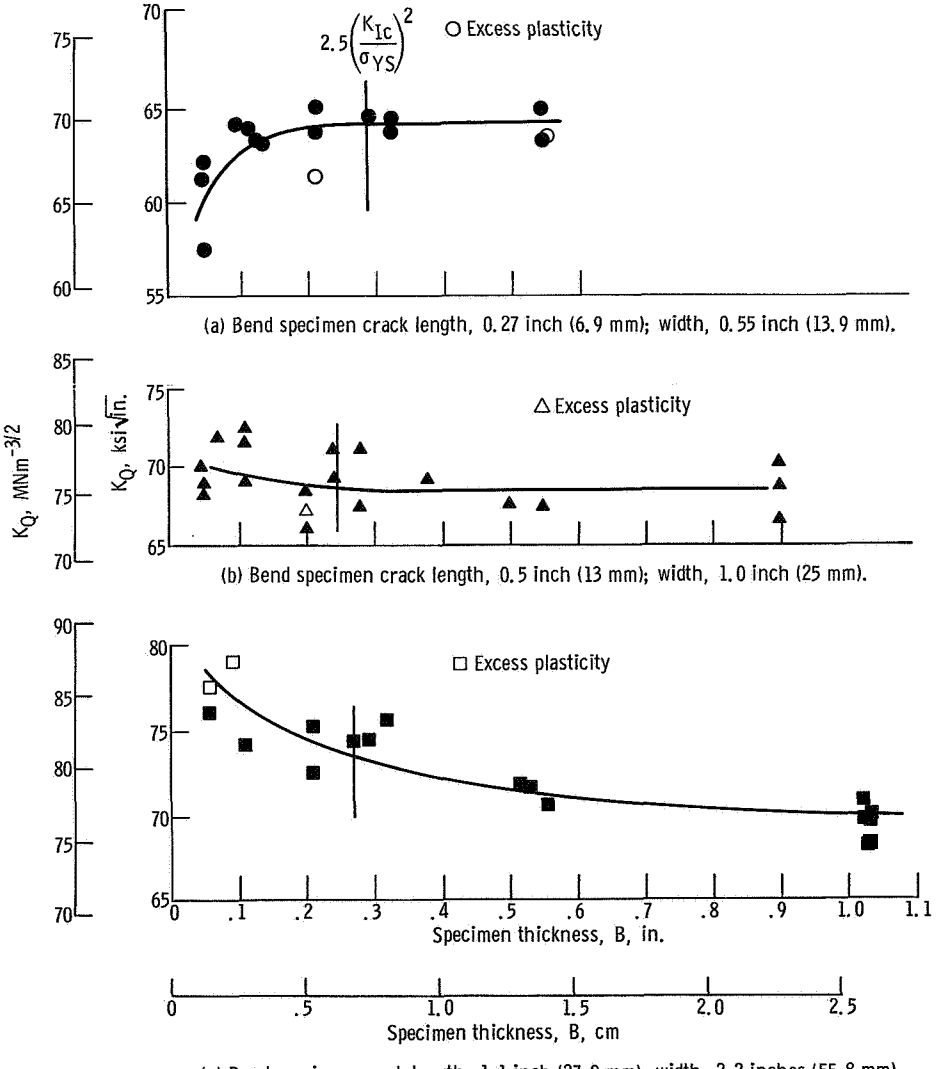

(a) Bend specimen crack length, 0.27 inch (6.9 mm); width, 0.55 inch (13.9 mm).

(b) Bend specimen crack length, 0.5 inch (13 mm); width, 1.0 inch (25 mm).

(c) Bend specimen crack length, 1.1 inch (27.9 mm); width, 2.2 inches (55.8 mm).

Figure 6. - K_Q values as function of specimen thickness for 4340 steel tempered at 750° F (672 K) for 1 hour. Conventional yield stress, 213 ksi (1467 MN/m^2).

For the shortest crack length (fig. 6(a)), the trend of K_Q is downward below a thickness which is somewhat smaller than that established by the size requirement. At the intermediate crack length (fig. 6(b)), the K_Q values are nearly independent of thickness over the entire range investigated, and a size requirement appears unnecessary. In contrast, for the longest crack length (fig. 6(c)), the K_Q values exhibit an upward trend at a thickness somewhat larger than that established by the size requirement. It is interesting to note (fig. 6(a)) that one test which met the size requirements would be rejected by the check procedure for excess plasticity.

The permissible range in thickness for bend specimens is restricted to $1 < W/B < 4$ by the E-24 Test Method. The effects of this limitation on the variation in valid K_{Ic} values produced by changes in crack length and thickness within the size requirements is illustrated in figure 7. This representation shows the trend curves from figure 6 which

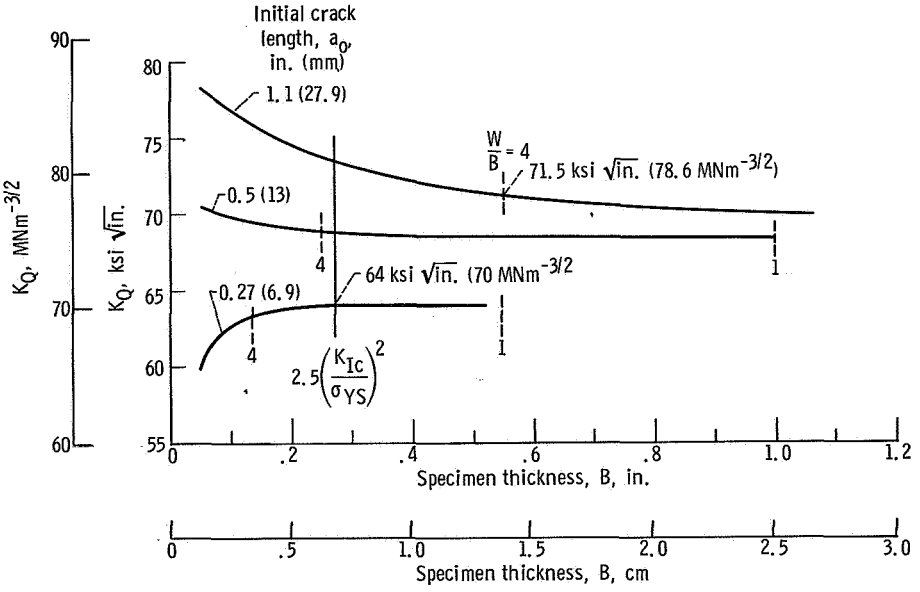

Figure 7. - Composite representation of the influence of specimen thickness on K_Q values for several crack lengths illustrating variation in plane-strain fracture toughness permitted by E-24 Test Method.

are marked to indicate the W/B limits. The variation in valid K_{Ic} values is about 12 percent of the lowest value.

Another source of variation in valid K_{Ic} values arises from the range in a/W permitted by the ASTM E-24 Test Method. The 5-percent secant slope of the present method corresponds to an apparent relative crack extension $\Delta a/a_o$ of 1.8 percent at an a/W of 0.5. For the permitted range of a/W between 0.45 and 0.55, the corresponding variation in $\Delta a/a_o$ will be from 2.1 to 1.6 percent. The resulting variation in K_{Ic} depends

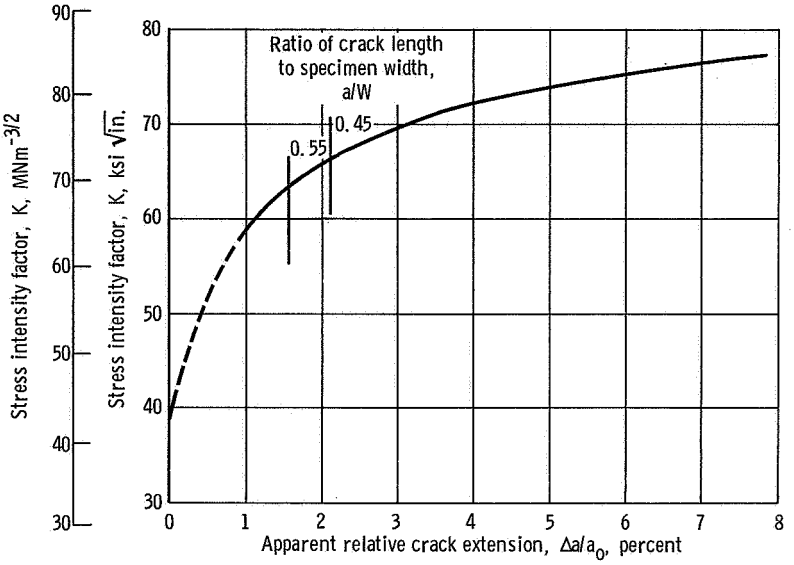

Figure 8. - Example of variation in plain strain fracture toughness with range of ratio of crack length to specimen width permitted by E-24 Test Method. Curve shown is typical for 0.27-inch- (6.9-mm-) thick bend specimens of 4340 steel tempered at 750° F (672 K) for 1 hour. Conventional yield strength, 213 ksi (1467 MN/m^2); specimen width, 0.55 inch (13.9 mm).

on the slope of the curve for K as a function of $\Delta a/a_o$. An example is given in figure 8 which shows a plot of K as a function of $\Delta a/a_o$ typical for the short crack length specimens having a thickness of 0.27 inch (6.9 mm). The vertical lines mark the permitted range of a/W, and, for the case selected, the variation in K_{Ic} is about 4.5 percent of the lowest value.

K_Q Values for 925° F (769 K) Temper Series

While only moderate effects of crack length and thickness were observed for valid K_{Ic} tests, very much larger effects can be encountered when using undersized specimens to test alloys with high ratios of $(K_{Ic}/\sigma_{YS})^2$. An example is the 4340 steel tempered at 925° F (769 K) (yield strength, 182 ksi (1255 MN/m^2)) which has a $(K_{Ic}/\sigma_{YS})^2$ of about 0.34 compared with about 0.11 for the 750° F (672 K) temper. The K_Q values for the 925° F (769 K) temper are shown in figure 9 as a function of crack length for thicknesses of 1 and 0.10 inch (25 and 2.5 mm), respectively. (The secant slopes were based on the actual a/W values of these specimens.) These data are supplemented with K_a values which have been calculated on the basis of loads corresponding to detection of continuous crack sounds.

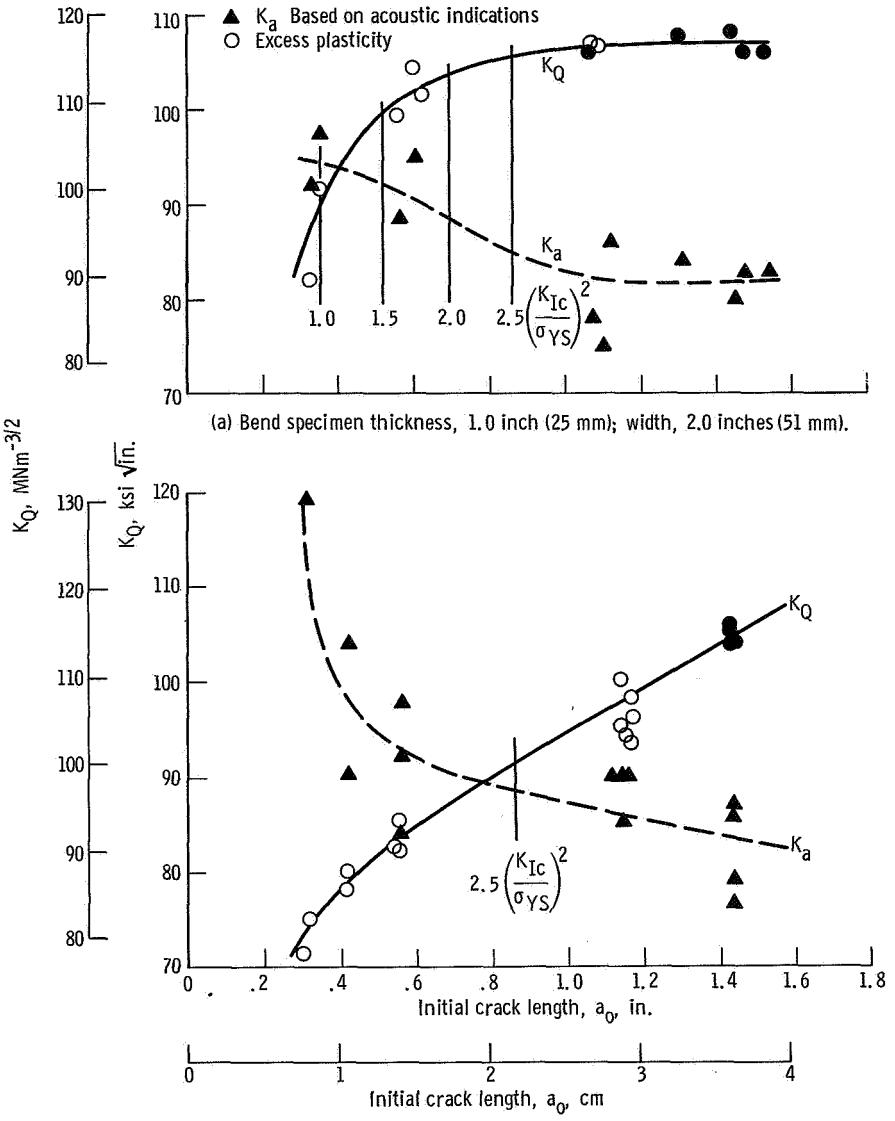

Figure 9. - K_Q and K_a values as function of crack length for 4340 steel tempered at 925° (769 K) for 1 hour. Conventional yield strength, 182 ksi (1253 MN/m^2).

The 1-inch- (25-mm-) thick specimens (fig. 9(a)) met the size requirements at crack lengths above about 0.85 inch (21.6 mm), and in this range $K_Q = K_{Ic}$ was essentially constant, as might be expected. At crack lengths below about 0.5 inch (13 mm), the K_Q values decrease rapidly; at the shortest crack length, $K_a > K_Q$, indicating that all the displacement at the load corresponding to K_Q was the result of plasticity at the crack tip. Those specimens with crack lengths shorter than that given by the size requirement did not pass the check procedures for excess plasticity. However, two tests with crack lengths exceeding the size requirement also did not pass this test. The several vertical

lines shown in figure 9(a) represent the K_Q values which would be measured if the size requirements were relaxed. For example, relaxing the crack length requirement to $1.0(K_{Ic}/\sigma_{YS})^2$ and dropping the check procedure for excess plasticity would give an apparent K_{Ic} value about 20 percent lower than the presently valid value. It should be noted that Steigerwald (ref. 7) has suggested the error in K_{Ic} due to relaxing the crack length requirement to $a = 1.0(K_{Ic}/\sigma_{YS})^2$ would be less than 5 percent.

The data for the 0.1-inch- (2.5-mm-) thick specimens (fig. 9(b)) involve extreme deviations from the size requirements and show a strong effect of crack length on the K_Q values over the entire range of crack length investigated. It is interesting to note that the K_Q value for sufficiently long cracks would exceed the K_{Ic} value for this alloy. For crack lengths below those given by the size requirement, $K_a > K_Q$, indicating that the K_Q values are not related to the fracture properties of the specimen. It is surprising to note that the specimens with the longest crack lengths passed the check procedure for excess plasticity, even though the thickness is only about an eighth of that required for a valid K_{Ic} test.

SCREENING TESTS FOR K_{Ic}

It would be advantageous if specimens considerably smaller than those required for a valid K_{Ic} test could be used to rate materials regarding their relative plane strain fracture toughness. A reduction in specimen size assumes particular importance in alloy development when the $(K_{Ic}/\sigma_{YS})^2$ ratios are high. A number of possible screening methods have been proposed including the use of precracked Charpy specimens and those based on correlation of standard Charpy impact energy values with valid K_{Ic} results. The present discussion is concerned with the possibility of simply using subsized specimens in otherwise standard K_{Ic} tests.

An opportunity to explore this possibility is available through a comparison of results of this investigation for 4340 steel with those obtained by Srawley (ref. 4) for a 250 grade maraging steel aged at various temperatures. This comparison may be made with the aid of figure 10(a), which presents K_Q data for both the 4340 steel and overaged conditions of the maraging steel as a function of yield strength. The range of valid K_{Ic} data for either alloy is shown by the shaded bands, and it is quite evident that the maraging steel exhibits a definite superiority in toughness at all yield strength levels investigated. The K_Q values for 0.5-inch- (13-mm-) thick specimens cut from the center of the thickness of the larger specimens are also shown in figure 10(a). These data for the 0.5-inch (13-mm) specimens do not represent valid K_{Ic} results. It should be noted that the K_Q values for the subsized specimens, based on a 5-percent secant intercept, would indicate the same toughness level for both steels at a yield strength of 180 ksi (1240 MN/m^2) and no increase in toughness when the yield strength is reduced from 200 to 180 ksi (1378 to

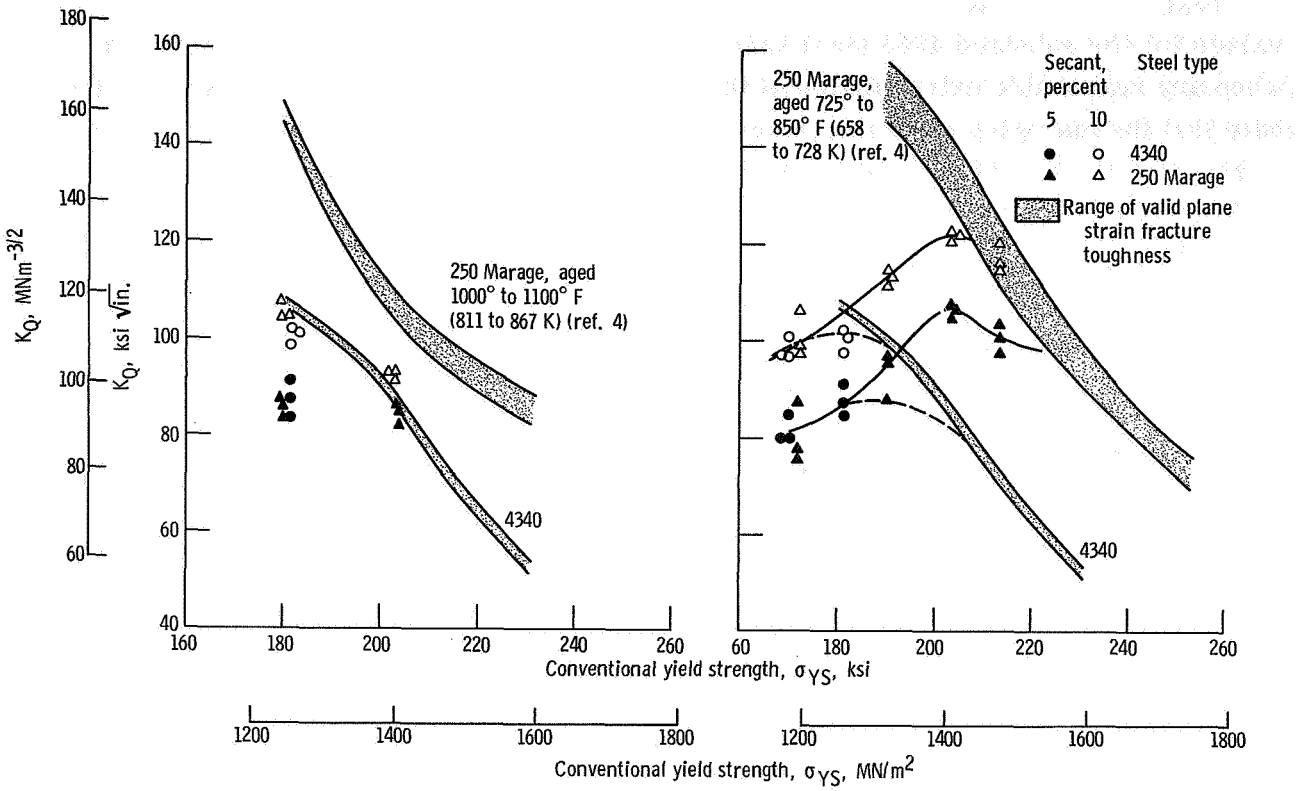

(a) 4340 and overaged 250 grade maraging steels.

(b) 4340 and underaged 250 grade maraging steels.

Figure 10. - K_Q values for subsized (0.5 in. (13 mm)) specimens and the range of valid plane strain fracture toughness as function of yield strength.

1240 MN/m^2). In contrast, the valid K_{Ic} values show an increasing superiority of the maraging steel with reduction in yield strength and continuously increasing values of K_{Ic} for both alloys with decreasing yield strength. It is interesting to note that, at a yield strength of 180 ksi (1240 MN/m^2), the subsized specimens were unable to distinguish the very large difference in K_{Ic} between the two steels even though $B(K_Q/\sigma_{YS})^{-2} = 2.2$. These results are further evidence against relaxing the size requirements.

An attempt was made to improve the usefulness of the subsized specimens by basing the K_Q values on a 10-percent rather than a 5-percent secant intercept. As shown in figure 10(a), this procedure raised all the values and restored the trend of increasing toughness with decreasing yield strength but did not separate the two alloys. It would have been interesting to explore the influence of further increasing the secant slope values; however, there was an insufficient number of tests on the maraging steel carried beyond the 10-percent secant load to permit a further analysis of this type.

A comparison similar to that shown in figure 10(a) may be made between the results of the underaged conditions of the maraging steel and those for the 4340 steel. The pertinent data are given in figure 10(b) and substantiate the observations made from fig-

ure 10(a). Thus, at the lowest yield strength level (170 ksi or 1172 MN/m^2), the K_Q values for the subsized 4340 steel specimens are equal to those for the maraging steel when any reasonable extrapolation of the trend curves for valid K_{Ic} values would indicate that the maraging steel is considerably superior in toughness. It is also interesting to note that the subsized specimens would rate the maraging steel to be tougher at a yield strength of 200 ksi (1378 MN/m^2) than at 190 ksi (1309 MN/m^2) when again the opposite is true for valid K_{Ic} values.

CORRELATION OF K_{Ic} WITH TENSILE PROPERTIES

Relations between smooth tensile properties and K_{Ic} are important not only to a basic understanding of fracture properties but in a direct engineering sense as well. Thus, they may offer means for estimating K_{Ic} values where specimen size requirements make plane strain fracture toughness tests impractical.

It is generally observed for a particular alloy that the strength of cracked specimens is inversely related to the tensile strength level when this level is varied by heat treatment, test temperature, or loading rate. Krafft and Sullivan (ref. 8) found their fracture toughness values for mild steel could be correlated with the upper yield strength to the -1.5 power when the test speed and temperature were varied. The K_{Ic} data for the 4340 steel tested in this investigation is shown in figure 11 plotted on a logarithmic scale against yield strength. These data are approximated fairly well by the relation $K_{Ic} = \sigma_{YS}^{-3}$ although the observed deviations from linearity are systematic and outside the range of data scatter. Added to figure 11 are Srawley's maraging steel data (ref. 4) representing both underaged and overaged conditions. For the underaged conditions (725° to 850° F or 658 to 728 K), the proportionality between K_{Ic} and yield strength is nearly the same as observed for the 4340 steel. On the other hand, the fully aged and overaged conditions do not follow any such simple relation, possibly because of appearance of a second aging reaction at temperatures between 850° and 950° F (728 and 783 K). Data showing the effect of temperature on tensile strength and K_{Ic} have been reported by Steigerwald (ref. 9) for several types of steels and a titanium alloy. Analysis of these data indicates that an inverse power relation between K_{Ic} and yield strength is approximated, but that the strength of the correlation varied among the alloys investigated. There is really no fundamental reason to expect such a simple relation between K_{Ic} and a strength value derived from a tensile test. However, the available data indicate that an inverse power relation can be useful for guidance in estimating K_{Ic} values where complex metallurgical effects are not dominant in determining the changes in tensile strength.

Both Krafft (ref. 10) and Hahn and Rosenfield (ref. 5) have proposed relations in which K_{Ic} is proportional to a strain-hardening index derived from the tensile test.

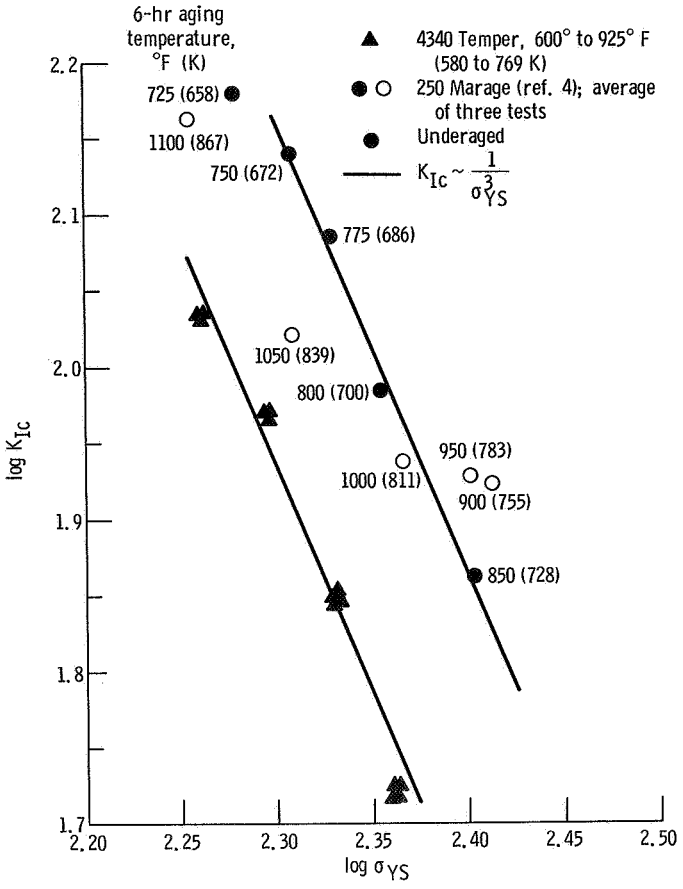

Figure 11. - Relation between plane strain fracture toughness and yield strength for 4340 and 250 grade maraging steels.

The relation proposed by Krafft includes a process zone size that would have to be determined by some independent means for the steel tested in this investigation. However, the relation proposed by Hahn and Rosenfield involves only quantities of stress and strain which can be determined directly from a tensile test. Thus,

$$K_{Ic} = \left(\frac{2}{3} E\sigma_{YS} n^2 \epsilon_f\right)^{1/2}$$

where E is Young's modulus, σ_{YS} the conventional yield strength, n the strain-hardening exponent, and ϵ_f the true strain at fracture. The constant 2/3 apparently has the dimension of a length.

One problem with these relations is the difficulty of arriving at a satisfactory definition of the strain-hardening index. Frequently this is defined as the exponent in the parabolic hardening law

$$\sigma = A\epsilon^n$$

where σ is the true stress and ϵ is sometimes taken as the total longitudinal true strain and sometimes as the plastic component of this strain. Unfortunately, as pointed out by Lauta and Steigerwald (ref. 11), many materials do not conform well to this law, and then n must be defined at some arbitrary strain. Under these circumstances, a strain-hardening index is unlikely to have general fundamental significance.

For the present analysis, the strain-hardening index n was taken as the strain value, where

$$\frac{d\sigma}{d\epsilon_{1p}} = \sigma$$

This is the well-known necking condition for uniaxial tension. The value of n for the various tempers of 4340 steel was obtained by graphic differentiation of the true stress against true longitudinal plastic strain curves.

It is possible to examine the usefulness of the relation proposed by Hahn and Rosenfield by employing it to predict the K_{Ic} values of the 4340 steel from the appropriate tensile data. The necessary information is shown in figure 12 as a function of the tempering temperature. The n values were obtained as described previously. These values are low and nearly constant between tempering temperatures of 600° and 850° F (589 to 728 K) and appear to be increasing at 925° F (769 K). The calculated K_{Ic} values differ widely from the valid data except at 600° F (589 K). It might be argued that the disagreement arises from the fact that 4340 does not follow power law hardening or that the n values are in error. In order to check these possibilities, plots of the logarithm of σ against the logarithm of ϵ_{1p} were made and the slopes of these compared with the n value determined from the instability condition. Examples of these plots are shown in figure 13 for tempering temperatures of 850° and 600° F (728 and 589 K), respectively. At 850° F (728 K) the logarithmic plot does exhibit a reasonably straight portion between $\epsilon_{1p} = 0.01$ and 0.1 with a slope essentially equal to n. This behavior was also observed for the 650° and 925° F (616 and 769 K) tempers. On the other hand, at 600° F (589 K) (fig. 13(b)), some imagination must be used to find a truly linear portion of the logarithmic plot. The line shown has a slope equal to the necking strain (n = 0.027). If the K_{Ic} value at 850° F (728 K) temper is used in Hahn and Rosenfield's relation to calculate n, a value of 0.06 is obtained. This is well outside the error in analysis of the curves of σ against ϵ_{1p} and, as shown in figure 13(a), represents a tangent to the curve for the logarithm of σ against the logarithm of ϵ_{1p} at a strain outside the range of uniaxial tension.

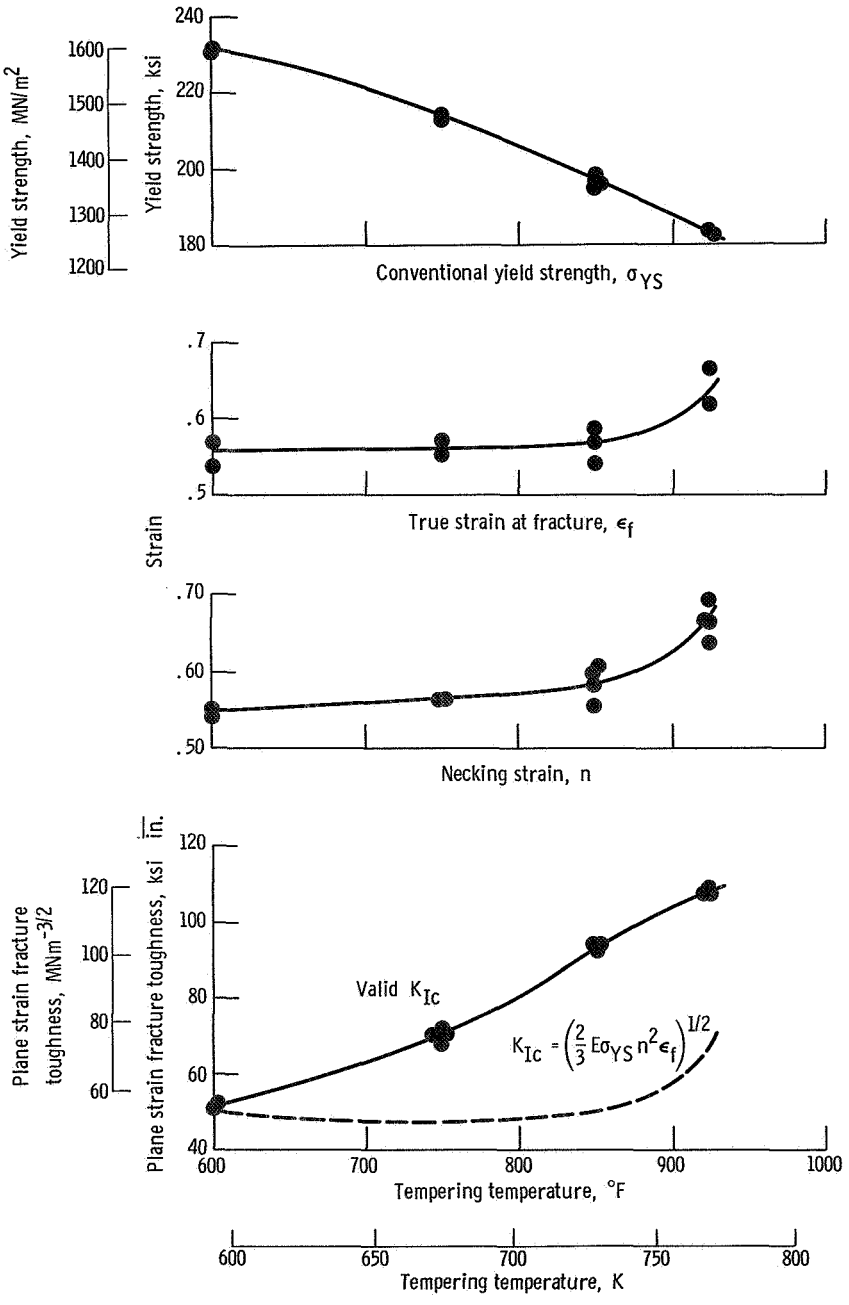

Figure 12. - Tensile properties and plane strain fracture toughness of 4340 steel as influenced by tempering temperature and a comparison between predicted and measured K_{Ic} values.

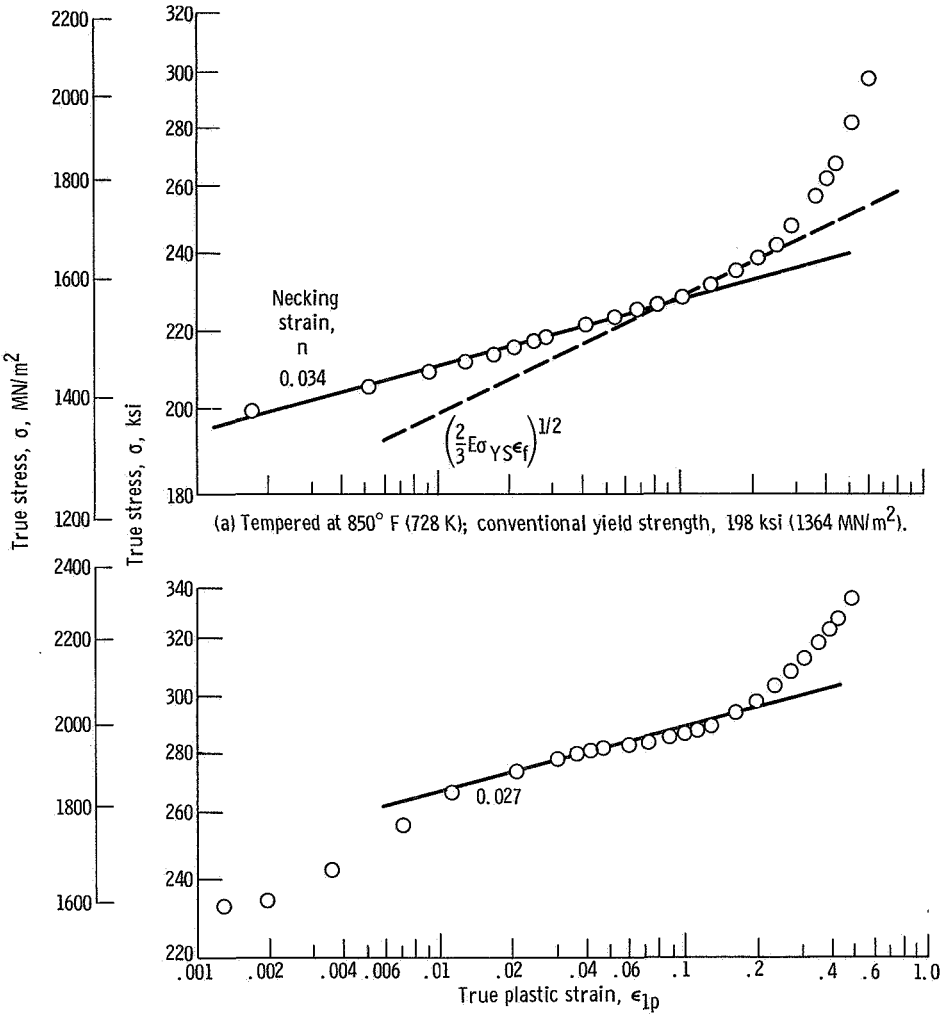

(a) Tempered at 850° F (728 K); conventional yield strength, 198 ksi (1364 MN/m^2).

(b) Tempered at 600° F (589 K); conventional yield strength, 213 ksi (1467 MN/m^2).

Figure 13. - True-stress - true-plastic-strain data for 4340 steel.

PRACTICAL SIGNIFICANCE OF RESULTS

Some features of the results which have practical significance to those engaged in fracture toughness testing are summarized as follows:

1. The value of K_{Ic} measured in accordance with the ASTM E-24 Test Method will vary somewhat with crack length and specimen thickness. This variation is inherent in the present definition of K_{Ic} and the tolerances placed on the specimen proportions. Its magnitude will depend on the material properties through their influence on crack growth resistance. For the steel tested in this investigation, the total variation was about 15 percent of the lowest value.

2. The variation in measured K_{Ic} values could be reduced by either increasing the

size requirements or basing K_{Ic} on a fixed increment of crack extension rather than on a percentage of the initial crack length. The first means is in harmony with the nature of elastic fracture mechanics but is otherwise unpopular. The second means would require a change in instrumentation to allow the sensitivity of crack extension measurements to be independent of specimen size. This might be accomplished by bucking out the elastic changes in displacement.

3. It is the opinion of the authors that the results of this investigation show that the present size requirements of $a = B \geqq 2.5(K_{Ic}/\sigma_{YS})^2$ are marginally sufficient to ensure the small scale yielding required by the basic elastic crack stress analysis and certainly should not be relaxed for engineering purposes. The results also show that tests to establish specimen size requirements can give misleading indications depending on the particular combination of specimen geometry and material properties selected.

4. When subsized specimens are tested using the E-24 Test Method procedures, the measured value K_Q is likely to be less than K_{Ic} if both the crack length and thickness are inadequate and can be greater than K_{Ic} if the specimen is undersize in thickness but oversize in crack length.

5. If procedures of the ASTM E-24 Test Method are used to determine K_Q values from subsized specimens which are intended for screening alloys regarding K_{Ic}, there is no assurance that the order in terms of K_Q will be that in terms of K_{Ic}. Furthermore, only rather small deviations from the size requirements can upset the rating order. On the basis of the presently reported results, there is no clear way of redefining K_Q to ensure its usefulness for screening purposes. However, further research is certainly desirable and should involve the analysis of complete (to maximum load) crack-growth-resistance curves for various sized specimens.

6. The check procedure for determining whether there has been at least 1-percent crack extension at K_Q will sometimes reject K_{Ic} results known to be valid. This is not surprising since crack growth may sometimes occur below $0.8\ P_s$. To the authors' knowledge, this difficulty with the check procedure is a minor problem and is not a reason for discarding it. One possibility of improving the situation would be to reduce the check load point from $0.8\ P_s$ to a lower value. This, however, would require increased precision in the autographic recording system that could best be obtained by bucking out the elastic displacement change. On the other hand, the check procedure could probably be eliminated entirely by doubling the size requirements.

7. For steels undergoing single aging or tempering reactions, useful guidance in estimating K_{Ic} values may in some cases be obtained by assuming $K_{Ic} \sim \sigma_Y^{-m}$. However, none of the proposed relations between uniaxial tensile properties and fracture toughness are sufficiently well developed to permit useful estimates of K_{Ic} from uniaxial tensile data alone.

Lewis Research Center,
National Aeronautics and Space Administration,
Cleveland, Ohio, June 21, 1969,
731-25-03-09-22.

APPENDIX A

DIMENSIONLESS DISPLACEMENT FACTOR

Values for the dimensionless displacement factor for three-point bend specimens were obtained by a boundary-value collocation method of elastic analysis (ref. 12) for a/W values between 0.2 and 0.8 in increments of a/W = 0.05. These results can be represented by the following polynominal

$$\log F = \log \frac{EvB}{P} = 3.48 + 12.7 \log \frac{a}{W} + 31.5 \left(\log \frac{a}{W}\right)^2 + 40.8 \left(\log \frac{a}{W}\right)^3 + 20.3 \left(\log \frac{a}{W}\right)^4$$

which fits within 2.5 percent for $0.2 < a/W < 0.8$. This is sufficient accuracy for the present purposes. However, if the function of a/W is to be differentiated, smoothing procedures must be used on the boundary-value-collocation data. Differentiation is necessary to obtain the H factors used in the ASTM E-24 Test Method to obtain the appropriate secant slopes.

APPENDIX B

ERRORS IN DETERMINATION OF CRACK GROWTH RESISTANCE FROM LOAD-DISPLACEMENT RECORDS

Errors in the curves for K as a function of Δa arise primarily from uncertainties in the value of the crack growth increment $\Delta a = a - a_o$ as determined from the load-displacement records. An estimate of this uncertainty may be made on the basis of the following assumptions: (1) the scale distance coordinates of P and v are about 4 and 2 inches (102 and 51 mm), respectively, on the autographic recorder paper; (2) a point on the autographic curve can be located within a 0.01-inch- (0.25-mm-) radius circle; and (3) the value of $a/W = 0.5$. For the conditions assumed, the error in v/P is

$$\frac{\Delta\left(\frac{v}{P}\right)}{\frac{v}{P}} = \frac{\Delta F}{F} = 0.006$$

where F is the dimensionless displacement function (see appendix A). When $\Delta(v/P) \ll v/P$,

$$\Delta\left(\frac{a}{W}\right) = F\frac{\Delta F}{F}\left[\frac{dF}{d\left(\frac{a}{W}\right)}\right]^{-1}$$

for an $a/W = 0.5$, $F = 36$, and $dF/d(a/W) = 200$. The differential was evaluated by an analysis of the boundary-value-collocation results for the dimensionless displacement factor (see appendix A).

On the basis of this analysis, the uncertainty in the reported values of Δa would be approximately 0.001 W inch (0.025 mm). Thus, the curves for K as a function of Δa (see figs. 4 and 5) are not established with a useful degree of accuracy near the origin. For the present purposes, it is considered that useful accuracy in Δa is obtained for values in excess of about 0.0025 inch (0.064 mm).

APPENDIX C

CALCULATION OF TRUE STRESS-STRAIN CURVES IN TENSION

The autographic load-elongation curves were reduced to true stresses and true plastic strains as follows: The total longitudinal strain e_{1t} was divided into an elastic and plastic part,

$$e_{1t} = e_{1e} + e_{1p}$$

which were determined directly from the load-elongation curves. The true longitudinal plastic strain is then

$$\epsilon_{1p} = \log_e(1 + e_{1p})$$

For values of $e_{1t} < 0.01$, the stresses were computed on the basis of the initial diameter. Otherwise the stresses were computed on the basis of true areas,

$$\sigma = \frac{P}{A} = \frac{4P}{\pi d_o^2}(1 + e_{3t})^{-2}$$

where $e_{3t} = e_{2t}$ is the total radial strain. (There was no detectable anisotropy.) The value of e_{3t} was taken as $e_{1t}/2$, where $0.01 < e_{1t} < 0.1$ and as

$$e_{3t} \approx \frac{1}{(1 + e_{1t})^{1/2}} - 1$$

where $e_{1t} > 0.1$. This procedure will give the true stresses within 1 percent.

In the case where the minimum specimen diameter was measured as a function of load, the true stresses could be determined directly from the diameter readings. The engineering radial plastic strain e_{3p} was computed as follows

$$e_{3p} = \frac{\Delta d}{d_o} + \frac{0.3\,\sigma}{E}$$

where σ is the true stress, Δd the diameter change (negative), and E the elastic modulus. For $\epsilon_{3p} < 0.05$,

$$\epsilon_{1p} = 2\epsilon_{3p} \approx 2e_{3p}$$

and for $e_{3p} > 0.025$

$$e_{1p} = (1 + e_{3p})^{-2} - 1$$

and

$$\epsilon_{1p} = \log_e(1 + e_{1p})$$

REFERENCES

1. Anon.: Proposed Method of Test for Plane-Strain Fracture Toughness of Metallic Materials. 1969 Book of ASTM Standards. Part 31. ASTM, 1969, pp. 1099-1117.

2. Brown, W. F., Jr.; and Srawley, J. E.: Plane Strain Crack Toughness Testing of High Strength Metallic Materials. Spec. Tech. Publ. No. 410, ASTM, 1967.

3. Srawley, J. E.; Jones, M. H.; and Brown, W. F., Jr.: Determination of Plane Strain Fracture Toughness. Mat. Res. & Standards, vol. 7, no. 6, June 1967, pp. 262-266.

4. Srawley, J. E.: Plane Strain Fracture Toughness Tests on Two-Inch Thick Maraging Steel Plate at Various Strength Levels. Proceedings Second International Conference on Fracture, Brighton, Sussex, England, 1969.

5. Hahn, G. T.; and Rosenfield, A. R.: Source of Fracture Toughness: The Relation Between K_{Ic} and the Ordinary Tensile Properties of Metals. Applications Related Phenomena in Titanium Alloys. Spec. Tech. Publ. No. 432, ASTM, 1968, pp. 5-32.

6. Jones, M. H.; and Brown, W. F., Jr.: Acoustic Detection of Crack Initiation in Sharply Notched Specimens. Mat. Res. & Standards, vol. 4, no. 3, Mar. 1964, pp. 120-129.

7. Steigerwald, E. A.: Crack Toughness Testing of High Strength Steels. Plane Strain Crack Toughness. Spec. Tech. Publ. No. 463, ASTM, 1969.

8. Krafft, J. M.; and Sullivan, A. M.: Effects of Speed and Temperature on Crack Toughness and Yield Strength in Mild Steel. ASM Trans., vol. 56, no. 1, Mar. 1963, pp. 160-175.

9. Steigerwald, Edward A.: Plane Strain Fracture Toughness for Handbook Presentation. TRW Equipment Labs. (AFML-TR-67-187, DDC No. AD-821626), July 1967.

10. Krafft, J. M.: Correlation of Plane Strain Crack Toughness with Strain Hardening Characteristics of a Low, a Medium, and a High Strength Steel. Appl. Mat. Res., vol. 3, no. 2, Apr. 1964, pp. 88-101.

11. Lauta, F. J.; and Steigerwald, E. A.: Influence of Work Hardening Coefficient on Crack Propagation in High-Strength Steels. Thompson Ramo Wooldridge, Inc. (AFML-TR-65-31, DDC No. AD-466448), May 1965.

12. Gross, Bernard; Roberts, Ernest, Jr.; and Srawley, John E.: Elastic Displacements for Various Edge-Cracked Plate Specimens. Int. J. Fracture Mech., vol. 4, no. 3, Sept. 1968, pp. 267-276.

"The aeronautical and space activities of the United States shall be conducted so as to contribute . . . to the expansion of human knowledge of phenomena in the atmosphere and space. The Administration shall provide for the widest practicable and appropriate dissemination of information concerning its activities and the results thereof."

—NATIONAL AERONAUTICS AND SPACE ACT OF 1958

NASA SCIENTIFIC AND TECHNICAL PUBLICATIONS

TECHNICAL REPORTS: Scientific and technical information considered important, complete, and a lasting contribution to existing knowledge.

TECHNICAL NOTES: Information less broad in scope but nevertheless of importance as a contribution to existing knowledge.

TECHNICAL MEMORANDUMS: Information receiving limited distribution because of preliminary data, security classification, or other reasons.

CONTRACTOR REPORTS: Scientific and technical information generated under a NASA contract or grant and considered an important contribution to existing knowledge.

TECHNICAL TRANSLATIONS: Information published in a foreign language considered to merit NASA distribution in English.

SPECIAL PUBLICATIONS: Information derived from or of value to NASA activities. Publications include conference proceedings, monographs, data compilations, handbooks, sourcebooks, and special bibliographies.

TECHNOLOGY UTILIZATION PUBLICATIONS: Information on technology used by NASA that may be of particular interest in commercial and other non-aerospace applications. Publications include Tech Briefs, Technology Utilization Reports and Notes, and Technology Surveys.

Details on the availability of these publications may be obtained from:

SCIENTIFIC AND TECHNICAL INFORMATION DIVISION

NATIONAL AERONAUTICS AND SPACE ADMINISTRATION

Washington, D.C. 20546